

Adsorption and Dissociation Reaction of Carbon Dioxide on Pt(111) and Fe(111) Surface: MO-study

Sang Joon Choe,* Dong Ho Park, and Do Sung Huh

Department of Chemistry, Inje University, Kim Hai 621-749, Korea

Received March 18, 2000

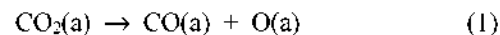
Comparing the adsorption properties and dissociation on a Pt(111) with that on a Fe(111) surface, we have considered seven coordination modes of the adsorbed binding site: di- σ , Δ , μ , π/μ , 1-fold, 2-fold, and 3-fold sites. On the Pt(111) surface, the adsorbed binding site of carbon dioxide was strongest at the 1-fold site and weakest at the π/μ -site. The adsorbed binding site on the Fe(111) surface was strongest at the di- σ site and weakest at the 3-fold site. We have found that the binding energy at each site that excepted 3-fold on the Fe(111) surface was stronger than the binding energy on the Pt(111) surface and that chemisorbed CO₂ bends because of metal mixing with $2\pi_u \rightarrow 6a_1$, CO₂ orbital. The dissociation reaction occurred in two steps, with an intermediate complex composed of atomic oxygen and π bonding CO forming. The OCO angles of reaction intermediate complex structure for the dissociation reaction were 115° on the Pt(111), and 117° on the Fe(111) surface. We have found that the CO₂ dissociation reaction on the Fe(111) surface proceeds easily, with an activation energy about 0.2 eV lower than that on the Pt(111) surface.

Introduction

In contrast to the extensive number of experimental and theoretical studies on the adsorption of CO on metal surface, adsorption of CO₂ has received little attention. Recently, groups^{1-8,9,11} have started to study the adsorption CO₂, using a variety of ultrahigh vacuum (UHV) surface science technique. CO₂ adsorption on metal surface is of particular interest because its role in a variety of reactions, including the Boudouart equilibrium and Fisher-Tropsch synthesis.¹⁻⁴ It has been reported⁹ that CO₂ has adsorbed on metal surfaces to form two states, one of which is a physisorbed linear CO₂ state and the other, a chemisorbed bent CO₂⁻ state. The chemisorbed anionic species turns out to represent an intrinsic precursor for CO₂ dissociation into CO and oxygen on Ni(100)³ and Fe(111)⁸ surfaces. Freund and co-workers⁹ arrived at theoretical representation of the three coordination modes of CO₂ on Ni atom. They found that the bonding between the CO₂ moiety and the metal atom is described best as a CO₂⁻ anion interacting with a Ni cation, they suggest that the electron transfer to CO₂ moiety drives the observed bent geometry of the coordinated CO₂ molecular and is accompanied by an elongation of the C-O bond distance with respect to the linear free molecule. They also address the correspondence between CO₂⁻ and metal-CO₂ vibration frequencies.⁹ Anderson¹⁰ calculated the theoretical binding energies, bond length of CO₂ and CO on a Cu(100) surface using the ASED-MO method. He suggests that the chemisorbed CO₂ bends because of metal d mixing with the $2\pi_u \rightarrow 6a_1$ CO₂ orbitals. Welder and co-workers⁵ found the bent anionic species to be stable up to 180 °K on the Fe(111) surface and identified it as the precursor to dissociation into adsorbed CO and atomic oxygen. At temperatures above room temperature the adsorbed CO formed by CO₂ dissociation undergoes dissociation into adsorbed carbon and oxy-

gen.⁸ Welder⁵ measured the initial heat of adsorption of CO₂ on polycrystalline iron film at 273 °K to be 2.91 eV/mol, much higher than that of CO, which was found to be 1.61 eV/mol. Thus, he suggests that this clearly points to dissociative adsorption of CO₂.

For the dissociation reaction,



Nassir¹¹ found that CO₂ is strongly chemisorbed on the Fe(100) surface and undergoes sequential carbon-oxygen bond cleavage. He proposes that the dissociation reaction occurs in two steps with an intermediate state composed of atomic oxygen and π -bonding CO forming.

This paper presents the results of a theoretical investigation into the mechanism of CO₂ dissociation reaction over Pt(111) and Fe(111). We calculate the binding sites of adsorbates, the binding energies, the charge transfer, the structure of CO₂ adsorption, the structure of reaction intermediate complex, and the activation energy for dissociation reaction.

Theoretical Method

In the present study, we used the atom superposition and electron delocalization molecular orbital (ASED-MO) theory.^{10,12-16,18,21-23} This technique has been used in previous studies of carbon monoxide adsorption on Pt((100)¹² and (111)¹⁶), and acetylene adsorption on Fe((100), (110), and (111)).²² The parameters used in the present study are in Table 1. The clusters used are assigned high spin, so that each d-band orbital contains at least one electron. Thus, lower levels in this band are doubly occupied, and some upper level are singly occupied. This gives the clusters approximately the bulk magnetic moment of iron. Our purpose for the present work is understanding the relative reactivities of clean Pt(111) and Fe(111) surfaces toward carbon

Table 1. Atomic Parameters; Principal Quantum Number (n), Valence State Ionization Potential (IP), Orbital Exponents (ζ) and Respective Coefficient (C) for d only; for all adsorption studies Pt and Fe ionization potentials are increased by 1.5 eV, and O and C ionization potentials are decreased by 1.5 eV; Further discussion in ref 23

Atom	s			p			d					
	n	Ip	ζ	n	Ip	ζ	n	Ip	C ₁	ζ_1	C ₂	ζ_2
C ^a	2	20.00	1.66	2	11.26	1.618						
O ^a	2	28.48	2.25	2	13.62	2.227						
Pt ^a	6	9.00	2.55	6	4.96	2.250	5	9.60	0.6567	6.013	0.5765	2.39
Fe ^b	4	7.87	1.70	4	4.33	1.40	3	9.00	0.5423	5.3500	0.6626	1.80

^aRef. 16. ^bRef. 23.

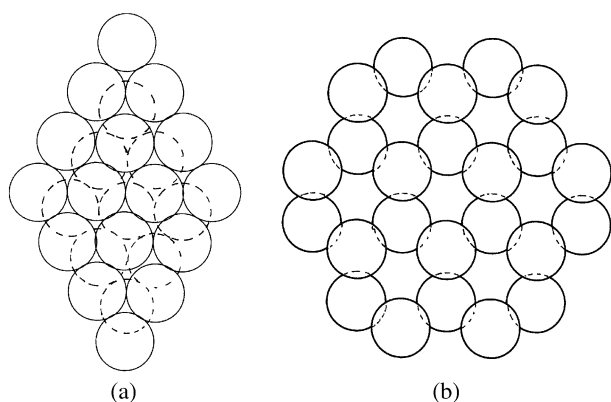


Figure 1. (a) 25-atom cluster model of Pt(111) is bulk superimposable with Pt-Pt nearest neighbor distance of 2.77 Å. (b) 24-atom cluster model of Fe(111) is open structure. Two metal atoms separated by 4.053 Å in a di- σ site.

dioxide, for which our model should be satisfactory. We plan to use clusters much larger than Pt₂₅ and Fe₂₄ in future studies of coverage dependent phenomena.

The ASFD-MO theory is a semiempirical approach for determining approximate molecular structures, force constants, bond strengths, electronic spectra, and reaction energy surfaces and orbitals, starting with experimental atomic valence ionization potentials and corresponding Slater orbitals. This theory identifies two energy terms for the chemical bond formation. One is a pairwise atom-atom repulsion energy called E_R . The other is an attractive energy due to electron delocalization by one-electron molecular orbital energy, EMO, which is obtained by diagonalizing a Hamiltonian similar to the extended Hückel Hamiltonian:

$$E = E_R + E_{MO}. \quad (2)$$

Pt atoms are in a face-centered cubic Bravais lattice and Fe atoms are body-centered cubic. For calculation on the metal surfaces we have modeled a metal cluster as shown in Figure 1. A bulk superimposable 25-atom cluster is used to model

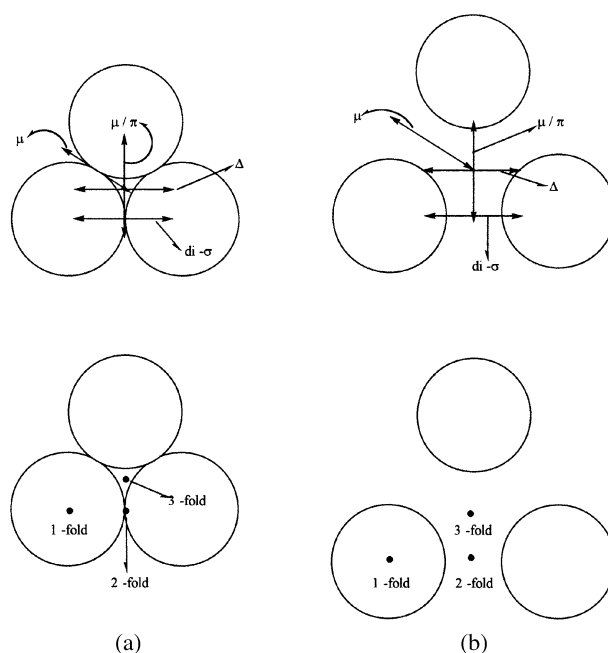


Figure 2. (a) Adsorption sites for CO₂ molecule studied on Pt(111). (b) Adsorption sites for CO₂ molecule studied on Fe(111).

the Pt(111). A 24-atom cluster, which is an open structure, is used to model the Fe(111). We considered seven coordination modes of binding sites as shown in Figure 2. Calculated bond distances, vibrational frequencies and dissociation energies for the CO₂ gas system are in reasonable frequencies with experimental results^{17,19,20} as shown in Table 2. To produce reasonable frequencies and charge transfers in this adsorption study, Fe and Pt ionization potentials^{17,23} were increased by 1.5 eV, and O and C ionization potentials were decreased by 1.5 eV as shown in Table 1.

Generally, a method that calculates the structures of a reaction intermediate complex considers two reaction pathways. One is the oxidation reaction pathway. The other is the dissociation pathway, which involves breaking the first CO

Table 2. Calculated Bond Lengths, Re. Harmonic Force Constants, ke. Dissociation Energies, De. Bond Angles, θ_e , and Bending Force Constants, k _{θ} for CO₂ gas state (Experimental Values are in Parenthes)

Molecules	State	Re (Å)	ke (m dyne/Å)	De (Kcal/mole)	θ_e (deg)	k _{θ} (m dyne/Å)
CO ₂	X ¹ Σ^+_{g}	1.14(1.16) ^a	17.87(16.8) ^a	—	180(180) ^a	1.33(0.393) ^a
CO ₂	¹ B ₂	1.23(—)	10.77	—	116(119 ^b , 122 ^c)	2.88

^aRef. 20. ^bRef. 19. ^cRef. 17.

bond in carbon dioxide. In this work, we calculated the structures of the reaction intermediate complex, using the first CO bond breaking in carbon dioxide. All of the angles are optimized to the nearest 1 full degree and the distance to the nearest 0.0 Å.

Results and Discussion

The calculated results for the adsorbed CO₂ on the Pt(111) and Fe(111) surface are given in Tables 3 and 4. On the di- σ , Δ , μ , and π/μ -site, we carried out the optimization by maintaining the O-C-O axis of carbon dioxide parallel to the surface at different heights and varying the C-O bond lengths of the CO₂ molecule and OCO angles away from the surface. On the 1-fold, 2-fold, and 3-fold site, we carried out the optimization by maintaining the vertical axis of carbon dioxide with one oxygen end down. For the platinum, the C-O bond lengths on the μ and π/μ -site are 1.16 Å, and they are 1.15 Å on the di- σ , Δ , 1-fold, 2-fold, and 3-fold site. On the μ and π/μ -site, the distorted carbon dioxide geometries in its gas phase put in the OCO angles within 4° from 180°. The geometry of carbon dioxide is most distorted at di- σ . The Pt-C distances from carbon of the adsorbed carbon dioxide to the platinum surface at each site are 2.12 Å, 1.91 Å, 2.91 Å, and 2.98 Å, respectively (see Figure 3). This Pt-C distance refers to the height. On the 1-fold, 2-fold, and 3-fold site, the adsorbed carbon dioxides are vertical with the O end

Table 3. Calculated Geometries and Binding Energies (BE) on the Pt(111) Surface and Fe(111)

Binding Site ^a	Geometries on the Pt(111) ^b			BE (eV)	Geometries on the Fe(111) ^c			BE (eV)
	θ (deg)	R (Å)	h (Å)		θ (deg)	R (Å)	h (Å)	
di- σ	146	1.15	2.12	1.35	164	1.14	1.42	3.73
Δ	158	1.15	1.91	0.23	164	1.14	0.86	3.04
μ	184	1.16	2.91	0.05	162	1.14	0.90	0.94
π/μ	182	1.16	2.98	0.04	164	1.14	1.05	2.77
1-fold*	180	1.15	1.70	1.70	180	1.15	1.50	2.48
2-fold*	180	1.15	1.25	0.93	180	1.14	0.06	1.91
3-fold*	180	1.15	0.98	0.88	180	1.15	0.80	0.66

*Geometry of adsorbed carbon dioxide: θ is OCO angle; R (Å) is CO bond length; h is the distances between carbon atom of CO₂ and the surface plane. *In case of 1-fold, 2-fold and 3-fold site, h is the distance between oxygen atom (O end down) of CO₂ and the surface; CO₂ is vertical with O atom end down. ^bSee Figure 2. ^cSee Figure 3. ^dSee Figure 4.

Table 4. Calculated Mulliken Overlap Populations and Charge (q) for the most favorable site of the Adsorbed Carbon Dioxide: The most favorable site on Pt(111) is 1-fold site and the site on Fe(111) is di- σ site

	Pt ₂₅ cluster	Fe ₂₄ cluster
M-C _{overlap} ^d	-0.15	-0.50
C-O _{overlap}	1.31	1.41
q	0.66	1.27

^dCalculated Mulliken Overlap Population between the surface model cluster and carbon atom in carbon dioxide.

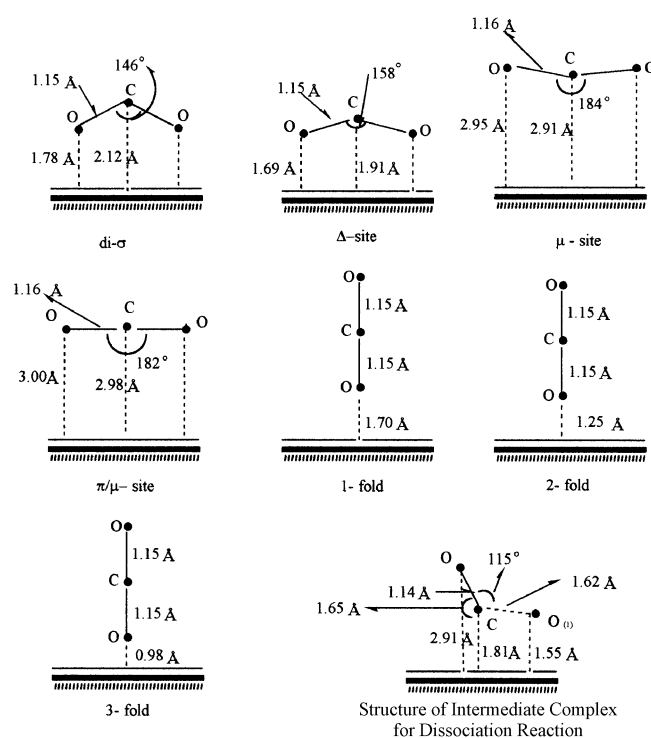


Figure 3. Structure details for CO₂ molecules on the Pt(111) surface.

down at each site. In this case, the Pt-O distances which refer to the height at each site are 1.70 Å, 1.25 Å, and 0.98 Å, respectively (see Figure 3). It can be seen that the adsorbed CO₂ molecule can occupy the di- σ , Δ , μ , π/μ -site, 1-fold, 2-fold, and 3-fold site. Their binding energies in Pt(111) are 1.35 eV, 0.23 eV, 0.05 eV, 0.04 eV, 1.70 eV, 0.93 eV, and 0.88 eV, respectively. The adsorption of carbon dioxide is strongest at the 1-fold site and weakest at the π/μ -site. The binding energy of the 1-fold site is in reasonable agreement with an earlier study¹² which was 1.76 eV for the Pt(100) surface. On the Fe(111) surface, the C-O bond lengths of carbon dioxide are 1.14 Å on the di- σ , Δ , μ , π/μ , and 2-fold site. The C-O bond lengths on the 1-fold and 3-fold site are 1.15 Å. The OCO angles are 164° for the di- σ , Δ , μ , π/μ , and 162° for the μ site. Those of the 1-fold, 2-fold, and 3-fold site are 180° (see Figure 4). The Fe-C distances, which refer to the height at each site, are 1.42 Å, 0.86 Å, 0.90 Å and 1.05 Å, respectively (see Figure 4). On the 1-fold, 2-fold, and 3-fold site, the adsorbed carbon dioxides are vertical, with the O end down at each site. In this case, the Fe-O distances from the O end down carbon dioxide to the platinum surface at each site are 1.50 Å, 0.06 Å, and 0.80 Å, respectively. This Fe-O distance refers to the height (see Figure 4). It can be seen that the adsorbed CO₂ molecule can occupy the di- σ , Δ , μ , π/μ , 1-fold, 2-fold, and 3-fold site. Their binding energies in the Fe(111) are 3.73 eV, 3.04 eV, 0.94 eV, 2.77 eV, 2.48 eV, 1.91 eV, and 0.66 eV, respectively. Adsorption of carbon dioxide is strongest at the di- σ site and weakest at the 3-fold site. Unfortunately, the binding energies at each sites are unknown for carbon dioxide. We were also interested in the initial heat of adsorption of carbon

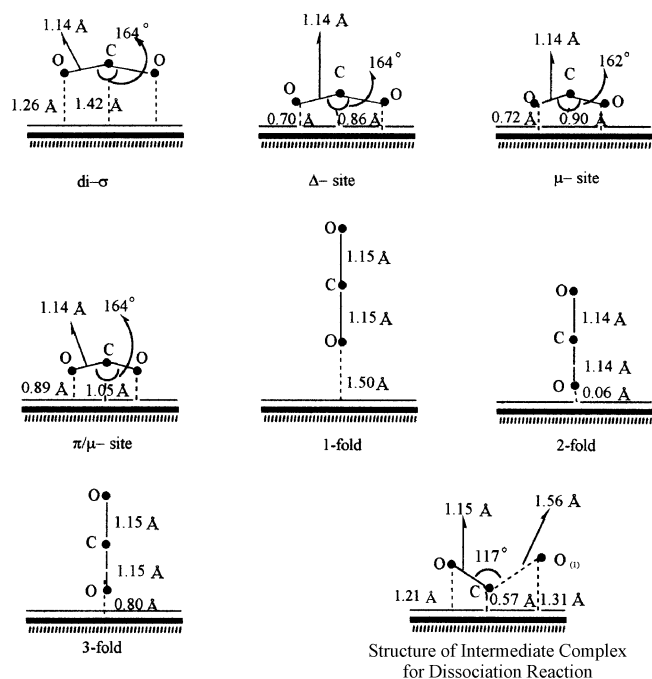


Figure 4. Structure details for CO_2 molecules on the Fe(111) surface.

dioxide on clean poly crystalline iron films at 273 °K. Because our parameter selection was done tentatively, the binding energies at each site may be a bit in error. It is interesting to note that the difference between the binding energy of the most favorite site and experimental value⁵ is about 20%. However, when we ignore the binding energy of μ -site and 3-fold, because it has a high deviation from the binding energy of di- σ site, the average value of the five sites, which is 2.79 eV, is in agreement with the experimental value,⁵ which is 2.91 eV. A Comparison the CO_2 bond distances for linear free CO_2 gas molecules (Table 2) with those for the 1-fold, 2-fold, and 3-fold, shows the C-O bond distance to be 0.01 Å elongated to the linear free gas state on Pt(111) surface. On iron surface, CO_2 bond distances are only 0.01 Å elongated at 1-fold and 3-fold. According to calculation, the CO_2 bond angle at di- σ , Δ , and π/μ is 164°. This result is in reasonable agreement with Anderson's suggestion¹⁰ that chemisorbed CO_2 bends because of metal d mixing with the $2\pi_{\mu} \rightarrow 6a_1$, CO_2 orbitals. Significantly, the 1B_2 excited state for CO_2 , with one electron excited from the $1\pi_g$ to the $2\pi_u$ orbital, bends to 116°, and adsorbed CO distances shrink 0.09 Å to equilibrium in Table 2. The result is that the electron from the surface metal transfers to the CO_2 moiety.⁹

Figure 5 shows the correlation diagram for CO_2 binding to a di- σ site of the Fe_{24} cluster and 1-fold site of the Pt_{25} cluster as shown in Figure 1. The hatched region at the top of the double filled band region indicates singly occupied orbital energy levels at the top of the bond. On the iron surface, chemisorbed CO_2 bends because of Fe_{s-d} band mixing with the $2\pi_{\mu} \rightarrow 6a_1$, CO_2 orbitals as shown in Figure 5. The binding in the chemisorbed molecule is a result of the participation of the $6a_1$ orbital in the bonding to the surface. On the

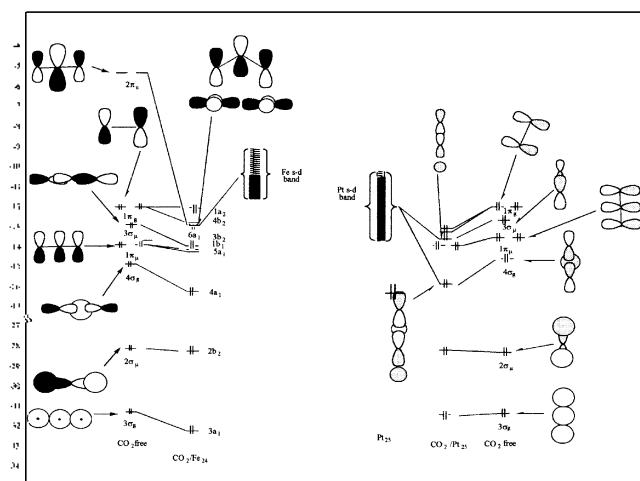


Figure 5. Orbital Pictures and energy level for free CO_2 and CO_2 adsorbed to metals surface. The energy levels for the carbon dioxide in linear free state are in the first and the sixth column. The second column is the energy levels for calculated carbon dioxide to the Fe(111) surface. The fifth column is adsorbed carbon dioxide to the Pt(111) surface.

platinum surface, chemisorbed CO_2 is stabilized by mixing with the Pt_{s-d} band. The $4\sigma_g$ is a lone pair orbital and it is binding to the platinum surface. As mention above, the binding energy at the 1-fold site is 1.70 eV for the Pt_{25} cluster and 3.73 eV at di- σ site for the iron surface. However, we have found that the binding energy is strongest at the di- σ site on the iron surface and at the 1-fold site on the platinum.

The next examination is the dissociation reaction. We have treated activation energy barrier change. It is the energy change from equilibrium of the most favorable site among seven coordination modes. For the platinum surface, as the C-O bond of the adsorbed carbon dioxide is stretched further from equilibrium in the one-fold site, dissociating into CO and O fragments with an activation barrier of 1.73 eV. For the iron surface, as the C-O bond of the adsorbed carbon dioxide is stretched further from equilibrium in the di- σ site, it dissociates into CO and O fragments with an activation barrier of 1.53 eV. We have compared the reduced overlap population of the adsorbed CO_2 molecule with that of the reaction intermediate complex in the CO_2 dissociation reaction. Table 4 shows the calculated Mulliken overlap population and charge for the most favorable site of adsorbed carbon dioxide. $M\text{-C}_{\text{overlap}}$ is the calculated Mulliken overlap population of Pt-C bond and Fe-C bond of the adsorbed carbon dioxide. $\text{C-O}_{\text{overlap}}$ is the calculated Mulliken overlap population of the C-O bond in adsorbed carbon dioxide. Table 5 shows the calculated results of the reaction intermediate complex in the dissociation reaction. It is of interest to note that (see Tables 4 and 5), on going from adsorbed reactants to the $[\text{CO}\cdots\text{O}_{(1)}]^*$ complex, the reduced overlap population of Pt-C and Fe-C increases while that of $\text{C}\cdots\text{O}_{(1)}$ decreases and that of other CO increases very slightly on the Pt_{25} cluster. That of other CO on the Fe_{24} cluster decreases very slightly. This can be attributed to the gradual strength-

Table 5. Calculated results of the Intermediate Complex for the Dissociation Reaction CO₂ ads → CO_{ads}-O_{ads} on a Pt(111) Surface and Fe(111) surface; C of CO₂ is at two-fold site

	Pt ₂₅ cluster	Fe ₂₄ cluster
Activation energy	1.73	1.53
M-C _{overlap} ^a	0.40	0.35
C-O _{overlap}	1.37	1.40
C···O ₍₁₎ overlap	0.35	0.46
q(C-O)	0.44	0.67
q(C···O ₍₁₎)	-0.17	-0.33
∠OCO(Degree) ^b	115	117
h(C) ^c	1.81	0.57

^aCalculated Mulliken Overlap Population between the surface metal cluster and carbon atom in the intermediate complex. ^bSee Figure 3 and 4. ^ch(C) is the distance between carbon of the intermediate complex and the surface.

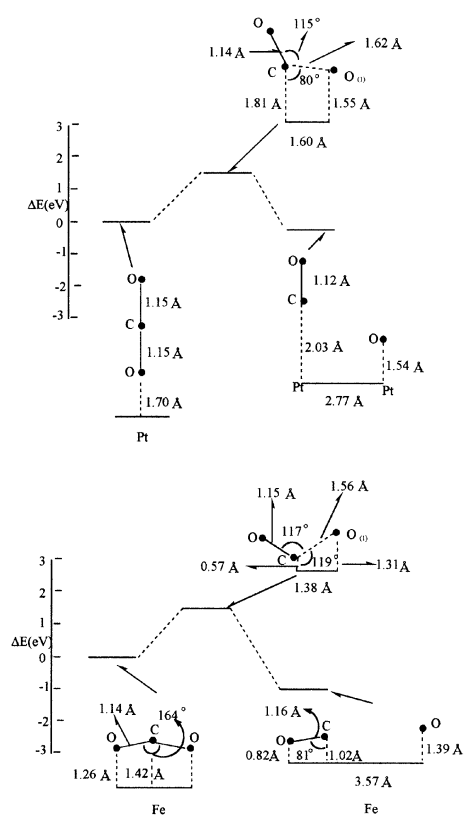


Figure 6. An energy versus reaction coordinate plot for the reactant studied. ΔE is the change for CO₂ passing through a complex, forming CO and O products over the Pt₂₅ and the Fe₂₄ cluster. On the platinum surface, CO₂, CO, and O are bound the one-fold site. On the Iron surface, CO₂ is bound to the di- σ site, and CO to a site which a center of adsorbed CO bond length is place on the center of the two metal atoms distance separated by 4.053 Å; CO is tilted by 99° from the surface normal.

ening of bonds for Pt-C bond and Fe-C bond in the dissociation reaction. The structures of the reaction intermediate complex are shown in Figures 3 and 4. Figure 6 shows plot of the energy versus the reaction coordinate. ΔE is the energy change for CO₂ dissociation passing through the reaction intermediate complex, forming the products CO and O over the Pt₂₅ cluster and Fe₂₄ cluster. On the platinum surface, the CO₂, CO and O are bound to the one-fold site. The reaction

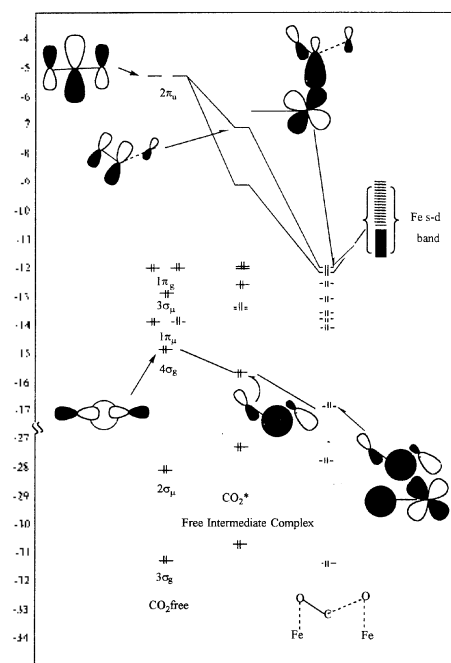


Figure 7. Orbital correlation diagram for dissociation reaction of carbon dioxide on the Fe(111). The [CO₂]* column of levels is a free reaction intermediate complex in which has surface removed.

intermediate complex is reached when CO adlayer of carbon dioxide is transformed to the two-fold site. On the iron surface, reactant CO₂ is bound to the di- σ site. Adsorbed CO forms of a bridge and center of the CO bond length is placed on the di- σ site which two metal atoms separated by 4.053 Å. The adsorbed CO is tilted by 99° from the surface normal. The oxygen atom is bound to the one-fold site. Figures 3 and 4. show the structure of reaction intermediate complex. The calculated OCO angle on the Pt₂₅ cluster is 115°, and it is 117° on the Fe₂₄ cluster. The distance of the C···O₍₁₎ is 1.62 Å for the platinum and 1.56 Å for the iron. The height that is referred to for the Pt-C distance is 1.81 Å for the platinum and 0.57 Å for the iron. The calculated activation energy of the reaction intermediate complex is 1.73 eV for the platinum and 1.53 eV for the iron surface. Orbital pictures and energy levels on the Fe₂₄ cluster are shown in Figure 7. The energy levels for the carbon dioxide are in the first column and those for the adsorbed dissociation reaction intermediate complex is in the third column. The second column is for a free complex structure in which the surface is removed. This column shows that the orbital is composed of atomic oxygen and π -bonding CO forming as was pointed out in ref 11. Compared with the carbon dioxide molecule, the energy in the free complex structure molecule increases by an average of 0.38 eV. Compared with adsorbed carbon dioxide on the Fe₂₄ cluster as shown in Figure 5, the energy in the complex, which is in the third column of Figure 7, increases on average by 0.22 eV. The result is largely due to the destabilization of the O-C-O orbital, which is caused by increasing the C···O₍₁₎ distance. The third column on the surface shows that these orbitals are stabilized by mixing with Fe_{s-d} band orbitals.

Conclusion

In the present study, we have arrived at the following results by using the ASED-MO theory.

The dissociation reaction occurs in two steps with an intermediate complex composed of atomic oxygen and the formation of π bonding CO forming.

a) The binding energy of carbon dioxide on the iron surface is stronger than that of platinum.

b) The binding energy of carbon dioxide is strongest at the 1-fold site on the Pt(111) surface and at the di- σ site on the Fe(111) surface.

c) The adsorbed structure are bent at the di- σ site on the Fe₂₄ cluster and the Pt₂₅ cluster.

d) The adsorbed structures are bent at the Δ -site, μ -site, and π/μ -site on the Fe(111) surface and nearly linear at the μ -site, π/μ -site on the Pt(111) surface.

e) CO₂ bond distances are elongated to the linear free gas state on Pt(111). On iron surface, CO₂ bond distances are elongated only at 1-fold and 3-fold.

f) The OCO angles of the reaction intermediate complex are 117° on the Fe₂₅ cluster and 115° on the Pt₂₅ cluster as shown in Figure 6.

g) The activation energy, which involves breaking the first CO bond in carbon dioxide, is 1.73 eV on the Pt(111) surface and 1.53 eV on the Fe(111) surface, respectively. CO₂ dissociation on the Fe(111) surface proceed less easily than on the Pt(111) surface.

Acknowledgment. The authors wish to acknowledge the financial support of the Korea Research Foundation made in the program year 1997.

References

1. Goodman, D. W.; Peebes, D. E.; White, J. M. *Surface Sci.* **1984**, *140*, L239.
2. Weinberg, W. H. *Surface Sci.* **1983**, *128*, L224.
3. Dubois, L. H.; Somorjai, G. A. *Surface Sci.* **1983**, *128*, L231.
4. Behner, H.; Spiess, W.; Wedler, G.; Borgmann, D. *Surface Sci.* **1986**, *175*, 276.
5. Korner, H.; Linder, H.; Welder, G.; Kreuzer, H. J. *Appl. Surface Sci.* **1984**, *18*, 361.
6. Wambach, J.; Odoref, G.; Freund, H. J.; Kuhlenbeck, H.; Neumann, M. *Surface Sci.* **1989**, *209*, 159.
7. D'Evelen, M. P.; Hamza, A. V.; Gdowski, G. E.; Madix, R. J. *Surface Sci.* **1986**, *167*, 451.
8. Freund, H. J.; Behner, H.; Bartos, B.; Wedler, G.; Kahlenbeck, H.; Neumann, M. *Surface Sci.* **1987**, *180*, 550.
9. Freund, H. J.; Messmer, R. P. *Surface Sci.* **1986**, *172*, 1.
10. Anderson, A. B. *Surface Sci.* **1977**, *62*, 119.
11. Nassir, M. H.; Dwyer, D. J. J. *Vac. Sci. Technol.* **1993**, *A11(4)*, 2104.
12. Choe, S. J.; Park, D. H.; Huh, D. S. *Bull. Korean Chem. Soc.* **1994**, *11*, 933.
13. Anderson, A. B.; Choe, S. J. J. *Phys. Chem.* **1989**, *93*, 6145.
14. Choe, S. J.; Park, S. M.; Park, D. H.; Huh, D. S. *Bull. Korean Chem. Soc.* **1993**, *14*, 55.
15. Choe, S. J.; Park, S. M.; Park, D. H.; Huh, D. S. *Bull. Korean Chem. Soc.* **1998**, *19*, 733.
16. Ray, N. K.; Anderson, A. B. *Surface Sci.* **1982**, *119*, 35.
17. Herzberg, G. *Molecular Spectra and Molecular Structure III. Electronic Spectra and Electronic Structure of Polyatomic Molecules*; Van Nostrand Reinhold Co.: New York., 1966.
18. Anderson, J. *Phys. Chem.* **1975**, *62*, 1187.
19. *CRC Handbook of Chemistry and Physics*; Weast, R. C., Ed.; CRC Press: Raton, FL., 1988; p F-169.
20. Smith, D. F.; Overend, J. J. *Chem. Phys.* **1971**, *55*, 1157.
21. Anderson, A. B. J. *Chem. Physics* **1976**, *64*, 4046.
22. Anderson, A. B.; Mehandru, S. P. *Surface Sci.* **1984**, *136*, 398.
23. Anderson, A. B. J. *Surface Sci.* **1981**, *105*, 159.